RSC Advances

PAPER

View Article Online
View Journal | View Issue

Cite this: *RSC Adv.*, 2017, **7**, 18491

Significantly enhanced electrochemical performance of a $ZnCo_2O_4$ anode in a carbonate based electrolyte with fluoroethylene carbonate†

Haibo Rong,[a] Zhongqing Jiang,[b] Si Cheng,[a] Bohong Chen,[a] Zihao Zhen,[a] Binglu Deng,[a] Yanmin Qin,[a] Guiting Xie,[a] Zhong-Jie Jiang *[a] and Meilin Liu *[ac]

The influence of fluoroethylene carbonate (FEC) as an additive to the conventional electrolyte of ethylene carbonate and dimethyl carbonate with lithium hexafluorophosphate on the electrochemical performance of the Li/$ZnCo_2O_4$ cell has been investigated. The addition of FEC is found to promote the formation of a more uniform and stable solid electrolyte interphase (SEI) layer with the thinner thickness on the surface of $ZnCo_2O_4$, which could reduce the charge transfer resistance and SEI resistance, increase the diffusivity of the lithium ions in the $ZnCo_2O_4$ electrode, and improve the stability of $ZnCo_2O_4$ during the repeated discharge/charge process. In addition, the formation of less LiF on the $ZnCo_2O_4$ surface could also be observed when FEC is added to the electrolyte, which decreases the interfacial impedance of the electrode materials. The Li/$ZnCo_2O_4$ cell in the electrolyte with FEC therefore exhibits substantially improved coulombic efficiency, reversible capacity, and long-term stability. The results make us believe that the addition of FEC could be a promising method to fabricate LIBs with improved performance.

Received 14th February 2017
Accepted 21st March 2017

DOI: 10.1039/c7ra01821e

rsc.li/rsc-advances

1. Introduction

Lithium-ion batteries (LIBs) have been widely used in consumer electronics.[1–4] However, the limited theoretical capacity of 372 mA h g^{-1} of the current commercial anode material of graphite has greatly hindered the application of LIBs in hybrid electric vehicles (HEVs), and electric vehicles (EVs) which usually require the uses of the LIBs with higher energy densities.[5–7] Numerous fundamental studies have therefore been devoted to developing alternative anode materials with higher theoretical capacity to enhance the energy densities of the LIBs.

Among various materials reported to date, transition metal oxides (TMOs) have attracted tremendous attention owing to their high theoretical capacity and energy density with great potential to replace the commercial graphite anode.[8–10] TMOs with binary metal ions have in particular shown higher electrochemical performance than their single component counterparts because of their complex chemical composition and the synergic effects between multiple metal species.[11–13] As reported recently, $ZnCo_2O_4$ could be used as promising anode materials for the LIBs due to its high reversible capacity, enhanced cycling stability, and environmental benignity.[14–16] Unfortunately, $ZnCo_2O_4$ suffers from large volumetric variation during the repeated Li^+ insertion/extraction process, leading to the high mechanical stress and breakdown of the conductive network of the electrode material.[17–19] As a result, $ZnCo_2O_4$ exhibits the low coulombic efficiency and inferior cycling performance due to its pulverization and detachment from the conductive additive and the current collector.[20,21]

Strategies frequently used to improve the electrochemical performance of the $ZnCo_2O_4$ based LIBs include nanostructuring of $ZnCo_2O_4$ and integrating it with carbonaceous materials such as carbon nanotubes (CNTs),[22] graphene,[23] and carbon cloth.[24] Nanostructuring could not only reduce the path for the Li^+ diffusion but also relax the strains caused by the volume variations during the repeated discharge/charge process.[25–27] Much work has demonstrated that nanostructured materials could exhibit substantially improved electrochemical performance when used in LIBs.[28–30] Nevertheless, the improvement of the electrochemical performance by nanostructuring is at the expense of the tap density of the electrode materials, which might not be a promising way to fabricate LIBs with both high energy and power densities.[31] Integration with carbonaceous materials, which enhances the electronic conductivity of the electrode materials, has been widely demonstrated to be a fascinating method to improve the electrochemical performance of the $ZnCo_2O_4$ based LIBs.[6,32] However, physical mixing of the $ZnCo_2O_4$ with carbonaceous materials might not be desirable since in this case the

[a]*New Energy Research Institute, College of Environment and Energy, South China University of Technology, Guangzhou 510006, Guangdong, China. E-mail: zhongjiejiang1978@hotmail.com; eszjiang@scut.edu.cn; Tel: +86-020-39381202*

[b]*Department of Materials and Chemical Engineering, Ningbo University of Technology, Ningbo 315016, Zhejiang, China*

[c]*School of Materials Science & Engineering, GA Institute of Technology, Atlanta, GA30332, USA. E-mail: meilin.liu@mse.gatech.edu; Tel: +1-404-894-6114*

† Electronic supplementary information (ESI) available: XRD pattern of the $ZnCo_2O_4$ particles. See DOI: 10.1039/c7ra01821e

improvement in the electrochemical performance of the LIBs is rather limited due to large interfacial resistance between $ZnCo_2O_4$ and carbonaceous materials. The complex synthetic procedures to prepare $ZnCo_2O_4$/carbon composites with specific structures to promote synergetic interactions between $ZnCo_2O_4$ and carbon are therefore required for obtaining LIBs with greatly improved performance,[33,34] which are indeed not time saving and usually fabricate the electrochemical materials with extremely low chemical yields. The additional method to improve the electrochemical performance of the $ZnCo_2O_4$ based LIBs is therefore of high interest.

Previous work has commonly reported that when anode operates at low potential close to that of metallic lithium, the reduction of the solvent and the salt of electrolyte, leading to the formation of surface film on the anode, also known as a solid electrolyte interphase (SEI) layer,[35–37] would occur. When the SEI layer accumulates to a certain thickness, the passivation of the anode prevents the further reduction of the solvent and the electrolyte salt. It has been widely demonstrated that the nature of the SEI layers formed on the anode surface plays an important role in the irreversible capacity and long-term stability of LIBs.[36] In the conventional carbonate-based electrolytes, the SEI layer consists mainly of insoluble reduction products, including lithium alkyl carbonates, lithium carbonate, ethers and polycarbonates.[21] This SEI layer may not be stable. The volume variations caused by the active electrode materials during the cycling processes could crack the SEI layer, resulting in the exposure of new SEI-free electrode materials to the electrolyte. This would lead to an extra consumption of the active Li^+ and the electrolyte solvents to form new SEI layer and the dissolution of the active materials by HF generated from the decomposition of the solvent and the electrolyte salt, resulting in the low cycling stability and reversible capacity of the LIBs.[38] In this sense, the formation of the stable SEI layer, which could endure the volume variations caused by the active materials during the cycling processes, could be an additional and the most economic and effective strategy to fabricate LIBs with improved electrochemical performance.[39–41]

Recent work has demonstrated that the addition of the organic additives with higher reactivity toward reduction to the conventional carbonate-based electrolytes is a promising method to fabricating LIBs with improved performance.[42–44] When the organic additives are selected to be capable of forming stable reduction products, their higher reduction reactivity would lead to the formation of SEI layer with improved stability prior to the reduction of the conventional carbonate-based electrolytes during the LIB cycling. Among various organic additive reported to date, fluoroethylene carbonate (FECs) has attracted tremendous attention. It has been used as a cosolvent and additive to carbonate-based electrolytes in the graphite and silicon based LIBs, and has demonstrated a variety of benefits on the electrochemical performance of LIBs.[45,46] Up to now, although FEC has been widely used as the additive to carbonate-based electrolytes in the graphite and silicon based LIBs, its influences on the electrochemical performance of the $ZnCo_2O_4$ based LIBs is less investigated. $ZnCo_2O_4$ is indeed a promising anode material, since it could be fabricated from earth abundant elements by more conventional synthetic methods, such as sol–gel and hydrothermal methods.

In this work, we therefore investigate the influences of FEC on the electrochemical performance of the $ZnCo_2O_4$ based LIBs. The results demonstrate that the addition of FEC would promote the formation of more uniform and stable SEI with the thinner thickness on the surface of $ZnCo_2O_4$. The thin and stable SEI could reduce the charge transfer resistance and SEI resistance, increase the diffusivity of the lithium ions of the $ZnCo_2O_4$ electrode, and improve the stability of $ZnCo_2O_4$ during the repeated discharge/charge process. In addition, the presence of FEC also leads to the formation of less LiF on the $ZnCo_2O_4$ surface. The Li/$ZnCo_2O_4$ cell in the electrolyte with FEC exhibits substantially improved electrochemical performance.

2. Experimental section

2.1 Chemicals

Zinc nitrate hexahydrate ($Zn(NO_3)_2\cdot 6H_2O$), cobalt nitrate hexahydrate ($Co(NO_3)_2\cdot 6H_2O$) and sucrose were obtained from Guangzhou Chemical Reagent Co. Ltd., battery-grade ethylene carbonate (EC), dimethyl carbonate (DMC), and lithium hexafluorophosphate ($LiPF_6$) were purchased from Dongguan Kaixin Battery Materials Co. Ltd. (China). Fluoroethylene carbonate (FEC) (>99.5%) was obtained from Fujian Chuangxin Technology Co. Ltd. (China). All the chemicals were used as received without further purification.

2.2 Preparation of the $ZnCo_2O_4$ particles

$ZnCo_2O_4$ used in this work was synthesized by a sucrose-assist combustion method. In brief, 5 mmol sucrose was dispersed in 20 mL deionized water. This was followed by addition of 3 mmol $Zn(NO_3)_2\cdot 6H_2O$ and 6 mmol $Co(NO_3)_2\cdot 6H_2O$. The obtained solution was heated to 90 °C under constant stirring to evaporate water. The resulting viscous precursor was dried at 70 °C overnight and further calcined at 600 °C under air atmosphere for 5 hours with a ramping rate of 2 °C min^{-1} to obtain the $ZnCo_2O_4$ particles.

2.3 Battery assembling

For the preparation of the working electrodes, the $ZnCo_2O_4$ particles, acetylene black (AB), and polyvinylidene fluoride (PVDF) binder (10 wt% in *N*-methyl-2-pyrrolidinone) with a mass ratio of $ZnCo_2O_4$: AB : PVDF = 7 : 2 : 1 were mixed. The obtained slurry was coated on a Cu foil, and dried at 120 °C under vacuum to remove the solvent. The electrode was then cut into disks with a mass loading of 2.0 mg cm^{-2}. The testing cells were assembled in a glovebox purged with high purity argon gas (the oxygen and water vapor levels in the glovebox maintained blow 1.0 ppm). Celgard 2400 were used as the separator, and the $ZnCo_2O_4$ particles and lithium metal were used as the working and counter electrodes, respectively. The electrolyte used was prepared by dissolving $LiPF_6$ into a 1 : 2 (v/v) mixed solution of EC and DMC to give a concentration of 1.0 M. To investigate the influence of FEC on the electrochemical performance of the Li/

$ZnCo_2O_4$ cells, 3.0% of FEC was added to the electrolyte and was allowed to dissolve overnight in a high pure argon-fill glove box (Mikrouna).

2.4 Electrochemical measurements

The cycling performance of the Li/$ZnCo_2O_4$ cells was evaluated on a Land cell test system (Land CT2001A, China) at various current densities within a cutoff potential window of 0.01 V and 3.0 V (*vs.* Li/Li^+) at room temperature. Cyclic voltammetric (CV) curves of the Li/$ZnCo_2O_4$ cells was collected on an Arbin testing system (BT2000, USA) at a scan rate of 0.1 mV s^{-1}. Electrochemical impedance spectroscopy (EIS) was acquired using a Zahner-elektrik IM6 electrochemical workstation in a frequency range of 10^5 to 0.01 Hz with an amplitude of 5 mV.

2.5 Preparation of the cycled electrodes for characterization

After electrochemical cycling, the cells were disassembled in the glovebox. The tested $ZnCo_2O_4$ electrodes and Li foils were rinsed with anhydrous DMC several times to remove residual solvent and $LiPF_6$ salt from the electrode surfaces and then dried before characterization. In all the cases, the cycled electrodes were exposed to air for less than 1 min during the sample preparation and transfer for characterization.

2.6 Characterization

The phase of the $ZnCo_2O_4$ particles was characterized by X-ray diffraction (XRD, Bruker D8 ADVANCE, Germany) with Cu K_α radiation. Morphologies of the electrode before and after cycling were examined on a scanning electron microscopy (SEM) (Merlin, German). Transmission electron microscopy (TEM) (JEM-2100HR, Japan) was used to investigate the microstructure of the surface layer on the $ZnCo_2O_4$ electrodes. Inductively coupled plasma mass spectrometry (ICP-MS) (Optima 8300, U.S.) was used to analyze deposited impurities on the lithium counter electrode and Zn^{2+} and Co^{2+} deposited on the lithium electrodes. Thermal behaviors of the $ZnCo_2O_4$ electrodes were analyzed on a thermal-gravimetric analysis (TGA) instrument (STA 449C, German) ramping of the temperature from room temperature to 400 °C. The chemical composition of the surface layer on the $ZnCo_2O_4$ electrodes was analyzed by X-ray photoelectron spectroscopy (XPS) (Phi X-tool instrument, Japan) with Al Kα as an X-ray source. All the obtained spectra were calibrated with hydrocarbon C 1s peak at 284.5 eV. Overlapping signals were analyzed using Gaussian–Lorentezian curve fit after the removal of a nonlinear Shirley background. ICP-MS (IRIS Intrepid II XSP, USA) was used to determine the contents of Zn and Co deposited on the cycled Li foils. Prior to the detection, the cycled Li foils were washed with DMC for three times and then dissolved in 2% HNO_3 solution, followed by adding deionized water to 25 mL.

3. Results and discussion

The $ZnCo_2O_4$ particles used in this work were synthesized by the sucrose-assist combustion method, as described in the Experimental section. These particles are well crystallized with a cubic spinel structure, as demonstrated by their X-ray diffraction (XRD) pattern in Fig. S1.† The absence of the diffraction peaks attributable to impurities and other phases indicates the high purity of the obtained product. These $ZnCo_2O_4$ particles were then used as the anode for assembling Li/$ZnCo_2O_4$ cells. The influences of FEC as the additive to the conventional electrolyte of EC and DMC with $LiPF_6$ on the electrochemical performance of the Li/$ZnCo_2O_4$ cells were investigated. Fig. 1a displays the cycling performance of the Li/$ZnCo_2O_4$ cells in the electrolytes with and without FEC. It shows that the reversible capacity of the Li/$ZnCo_2O_4$ cell in the electrolyte without FEC is 732.2 mA h g^{-1} for the initial cycle, which gradually increases to 847 mA h g^{-1} (because of the gradual activation of more active sites available to the Li^+ storage) when the cell is discharged/charged for 50 cycles. The further increase of the cycle number leads to a continuous reduction of the reversible capacity with only 48.5% of the maximum reversible capacity preserved for the cell discharged/charged for up to 200 cycles, indicating a relatively poor cycling stability of the Li/$ZnCo_2O_4$ cells in the electrolyte without FEC. This could also be demonstrated by its coulombic efficiency shown in Fig. 1b. As shown in Fig. 1b, in the absence of FEC the initial coulombic efficiency of the Li/$ZnCo_2O_4$ cell is 72.5%. Although it could be increased to ~98% with increase of

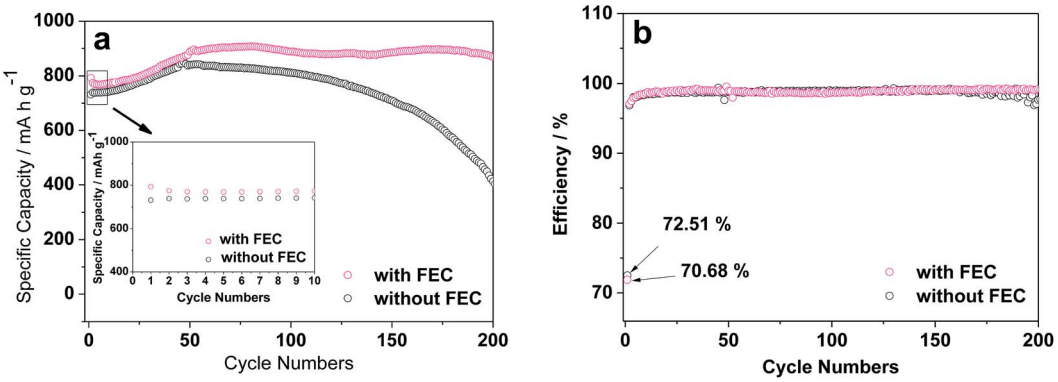

Fig. 1 Cycling performance (a) and coulombic efficiency (b) of the Li/$ZnCo_2O_4$ cells in the electrolytes with and without FEC at the current density of 200 mA g^{-1}. Cycling performance of the Li/$ZnCo_2O_4$ cells in the electrolytes with and without FEC at the first 10 cycles is shown in (a).

the cycle number, further increase of the cycle number would lead to its gradual decrease. The addition of FEC could significantly improve the reversible capacity and stability of the Li/$ZnCo_2O_4$ cell. As shown in Fig. 1b, although the initial coulombic efficiency of the Li/$ZnCo_2O_4$ cells in the presence of FEC (~70.7%) is slightly lower than that of the Li/$ZnCo_2O_4$ cells in the absence of FEC, increase of the cycle number would lead to a stable coulombic efficiency of ~98% even when the Li/$ZnCo_2O_4$ cell is discharged/charge for up to 200 cycles. Furthermore, the initial reversible capacity of the Li/$ZnCo_2O_4$ cell in the electrolyte with FEC is 792.8 mA h g^{-1}, which is much higher than that of the Li/$ZnCo_2O_4$ cell in the electrolyte without FEC, as shown in Fig. 1a. Although a slight decrease of the reversible capacity could be observed in the first four cycles (mainly due to the irreversible reduction of FEC, which increases the energy consumed in the discharge process), further increase of the cycle number lead to gradual increase of the reversible capacity and a relatively stable reversible capacity is achieved when the Li/$ZnCo_2O_4$ cell in the electrolyte with FEC is discharged/charged for up to 60 cycles. Worthnoting is that the reversible capacity of the Li/$ZnCo_2O_4$ cell in the electrolyte with FEC is always higher than that of the Li/$ZnCo_2O_4$ cell in the electrolyte without FEC over the cycling, as shown in Fig. 1a. These results clearly demonstrate that the addition of FEC could greatly improve the electrochemical performance of the Li/$ZnCo_2O_4$ cells.

Indeed, the improvement of the electrochemical performance of the Li/$ZnCo_2O_4$ cells by the addition of FEC could further be demonstrated by their higher rate capacities. As shown in Fig. 2, the reversible capacities of the Li/$ZnCo_2O_4$ cells in the electrolytes with FEC are 640, 580.6, 517.9, 478.1, 456.4 and 442.9 mA h g^{-1} at the current densities of 0.5, 1.0, 2.0, 3.0, 4.0 and 5.0 A g^{-1}, respectively, which are much higher than those of the Li/$ZnCo_2O_4$ cells in the electrolytes without FEC (the reversible capacities of the Li/$ZnCo_2O_4$ cells in the electrolytes without FEC are 598.8, 485.2, 391.8, 344.8, 302.5 and 283.6 mA h g^{-1} at the respective current densities of 0.5, 1.0, 2.0, 3.0, 4.0 and 5.0 A g^{-1}). The higher rate capacities may suggest that the addition of FEC enhances the lithiation/delithiation kinetics of the $ZnCo_2O_4$ electrode, which decreases the overall polarization of the Li/$ZnCo_2O_4$ cells, leading to their improved electrochemical performance.

To understand the influence of FEC on the electrochemical behaviors of the Li/$ZnCo_2O_4$ cells, the CV curves of the $ZnCo_2O_4$ electrode in the electrolytes with and without FEC were investigated. Fig. 4 shows that in the both cases the CV curves of the $ZnCo_2O_4$ electrode exhibit two cathodic and two anodic peaks at the first cycle, consistent with the electrochemical reactions associated with the discharge and charge processes of the $ZnCo_2O_4$ based anode in LIBs shown in Fig. 3. The sharp cathodic peak could be assigned to the reduction of $ZnCo_2O_4$ to Zn and Co (eqn (1) in the Fig. 3), accompanied by the decomposition of the organic electrolyte to form a solid electrolyte interphase (SEI) layer. The small peak at 0.36 V is ascribable to the formation of Li/Zn alloy (eqn (2) in the Fig. 3). The anodic peaks appearing at 1.76 and 2.15 V could be attributed to the oxidation of Co to Co^{3+} and Zn to Zn^{2+} (eqn (3)–(5) in the Fig. 3), respectively. At the subsequent cycles, the sharp cathodic peaks in the CV curves of the $ZnCo_2O_4$ electrode in both the electrolytes with and without FEC are shifted to higher voltage potentials, indicating the irreversibility of the reduction of $ZnCo_2O_4$ and the decomposition of the organic electrolyte. This is in good agreement with the lower initial coulombic efficiencies of the Li/$ZnCo_2O_4$ cells in both the electrolytes with and without FEC, as shown in Fig. 1b. The overlapping of the anodic and cathodic peaks in the subsequent cycles indicates improved stability and cyclability of the insertion and extraction of lithium ions in the anode with increase of the cycle numbers, consistent with the improved Coulombic efficiencies of the Li/$ZnCo_2O_4$ cells in both the electrolyte with and without FEC after the first cycles (Fig. 1b). The most interesting is that except for the sharp cathodic peak at the first cycle, the other peaks in the CV curves of the $ZnCo_2O_4$ electrode in the electrolytes with and without FEC show the relatively similar shape profiles and voltage potentials. As shown in Fig. 4, in the presence of FEC,

$$ZnCo_2O_4 + 8Li^+ + 8e^- \rightarrow Zn + 2Co + 4Li_2O \quad \text{Eq. 1}$$

$$Zn + Li^+ + e^- \leftrightarrow LiZn \quad \text{Eq. 2}$$

$$Zn + Li_2O \leftrightarrow ZnO + 2Li^+ + 2e^- \quad \text{Eq. 3}$$

$$2Co + 2Li_2O \leftrightarrow 2CoO + 4Li^+ + 4e^- \quad \text{Eq. 4}$$

$$2CoO + 2/3Li_2O \leftrightarrow 2/3Co_3O_4 + 4/3Li^+ + 4/3e^- \quad \text{Eq. 5}$$

Fig. 3 Electrochemical reactions associated with the discharge and charge processes of the $ZnCo_2O_4$ based anode in LIBs.

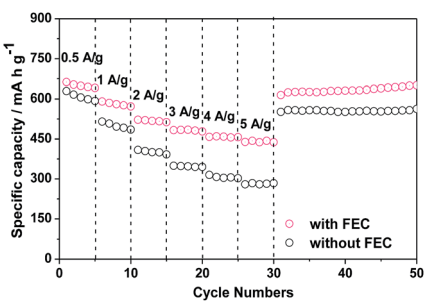

Fig. 2 Rate capacities of the Li/$ZnCo_2O_4$ cells in the electrolytes with and without FEC.

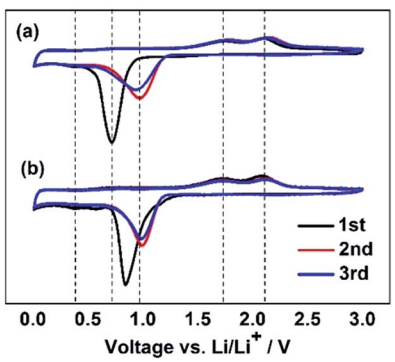

Fig. 4 CV curves of the Li/$ZnCo_2O_4$ cells in the electrolyte without (a) and with (b) FEC.

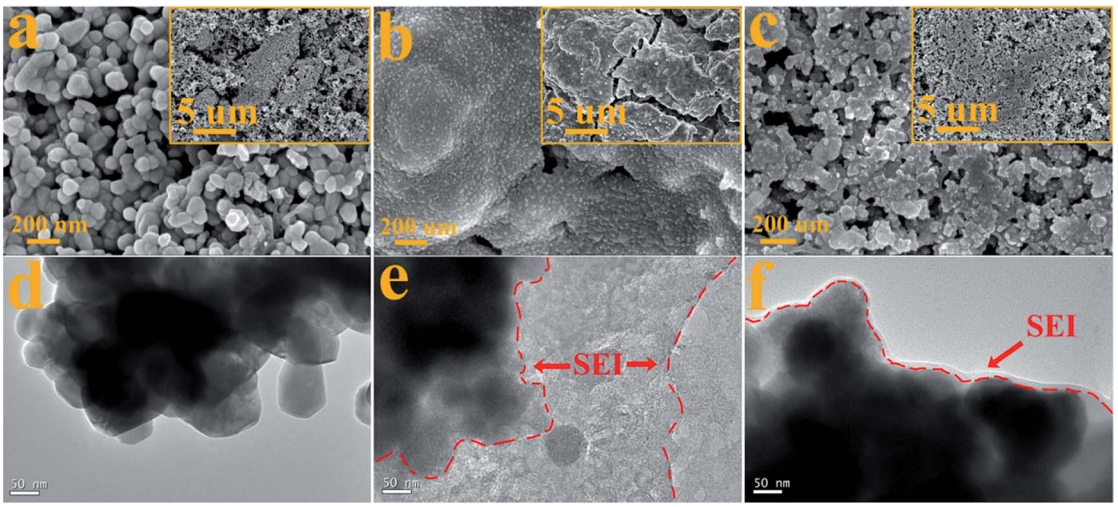

Fig. 5 (a)–(c) SEM images of the pristine $ZnCo_2O_4$ electrode (a) and the $ZnCo_2O_4$ electrodes after 200 discharge/charge cycles in the electrolyte without (b) and with FEC (c). The insets in the figures are their corresponding SEM images with the low magnification. (d)–(f) TEM images of the pristine $ZnCo_2O_4$ (d) electrode and the $ZnCo_2O_4$ electrodes after 200 discharge/charge cycles in the electrolyte without (e) and with FEC (f). The SEI layers on the surfaces of the cycled $ZnCo_2O_4$ electrodes are marked in (e) and (f).

the sharp cathodic peak in the first cycle of the CV curve appears at the relatively high peak potential and exhibits a different shape profile. Since the CV curves were recorded strictly in the same experimental condition in the both cases, we would attribute the appearance of the sharp cathodic peak with the different shape and voltage potential in the first cycle of the CV curve of the $ZnCo_2O_4$ electrode in the electrolyte with FEC to the reduction of FEC. This is consistent with the previous reports that reduction of FEC occurs at the potential higher than those of EC and DMC.[47,48] The reduction of FEC would suppress the reduction of EC and DMC and might facilitate the formation of the SEI layer on the surface of the anode with morphology and composition different from that formed from the electrolyte in the absence of FEC. The results here make us believe that the addition of FEC does not change the Li-ion storage mechanism of the $ZnCo_2O_4$ electrode, but alters the SEI layer on the surface of the electrode materials.

To demonstrate the reduction of FEC and the formation of the SEI layer on the surface of the $ZnCo_2O_4$ electrode, the morphologies of the pristine $ZnCo_2O_4$ electrode and the $ZnCo_2O_4$ electrodes after 200 cycles in the electrolytes without and with FEC were measured. The SEM image of the pristine $ZnCo_2O_4$ electrode in Fig. 5a shows the homogeneous distribution of the $ZnCo_2O_4$ particles with an average diameter of ~100 nm. This is consistent with its TEM image in Fig. 1d, where the $ZnCo_2O_4$ particles with the average diameter of ~100 nm are clearly observed. After 200 cycles in the electrolyte without FEC, the $ZnCo_2O_4$ electrode is fully covered with no granular-like particles observed (Fig. 5b), indicating the inhomogeneous formation of the SEI layer from the reduction of EC and DMC. This could further be demonstrated by its TEM image in Fig. 5e, where the agglomerated $ZnCo_2O_4$ particles coated with non-uniform and rough shell could be observed. The formation of the agglomerated particles might indicate the occurrence of the particle aggregation and fusing during the repeated discharge/charge process. As reported previously, the SEI layers formed in the electrolyte of EC and DMC are not stable and the repeated insertion and extraction of lithium ions would lead to aggregation and significant change in the particle dimensions of the electrode materials.[49] The low magnification SEM image in the inset of Fig. 5b shows the presence of cracks on the surface of the $ZnCo_2O_4$ particles, which might be formed from the volume variations of the electrode materials during the repeated discharge/charge. The formation of these cracks would lead to the exposure of new SEI-free $ZnCo_2O_4$ surface to the electrolyte, resulting in the further formation of the SEI layer. This is consistent with the result in Fig. 1b, which shows that the Li/$ZnCo_2O_4$ cell in the electrolyte without FEC exhibits the slightly reduced coulombic efficiency when discharged/charged up to 200 cycles. Analysis of the $ZnCo_2O_4$ electrode cycled in the electrolyte with FEC shows less severe morphological change to

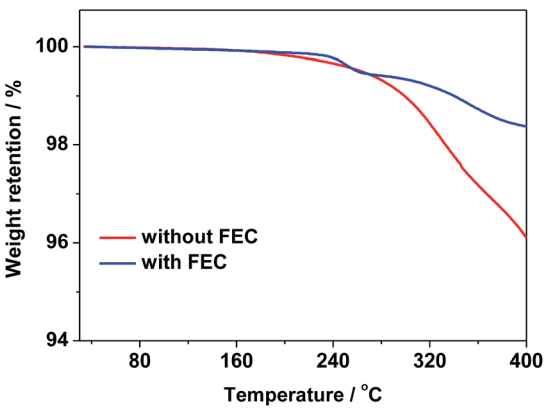

Fig. 6 TGA profiles of the $ZnCo_2O_4$ electrodes after 200 cycles in the electrolytes with and without FEC.

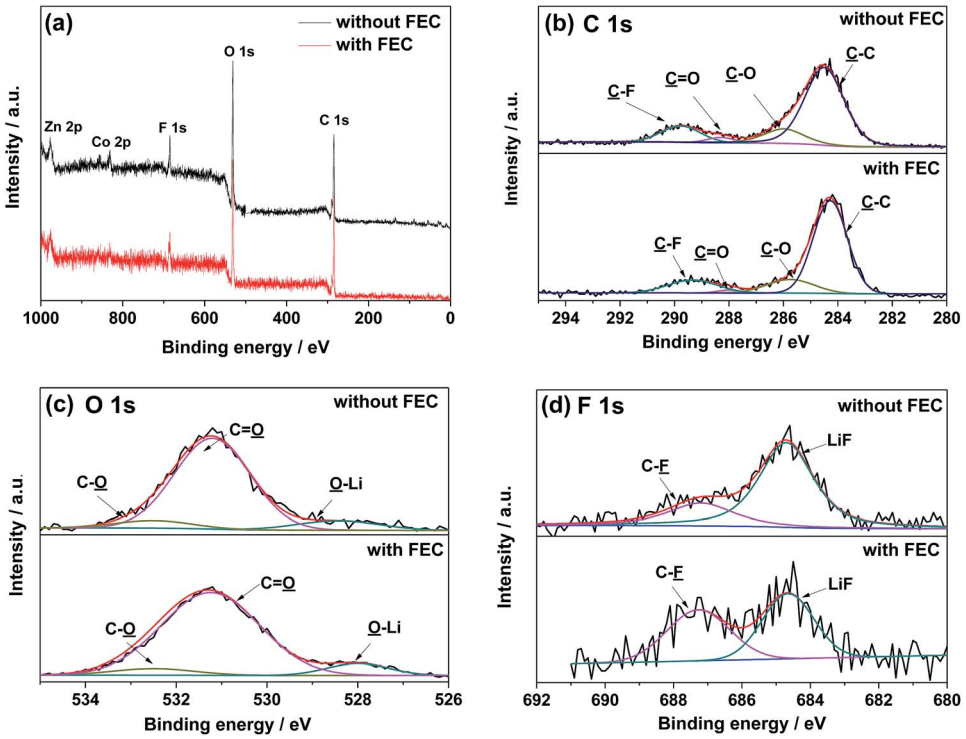

Fig. 7 (a) XPS survey spectra of the $ZnCo_2O_4$ electrodes cycled in the electrolyte with and without FEC. (b) Deconvoluted C 1s, (c) deconvoluted O 1s, and (d) deconvoluted F 1s spectra of the $ZnCo_2O_4$ electrodes cycled in the electrolyte with and without FEC.

the particles. As shown in Fig. 5c, the granular-like particles with slightly larger sizes could be observed in the sample cycled in the electrolyte with FEC, and the original morphology of the pristine sample was much better preserved. The TEM image in Fig. 5f shows the formation of uniform and thin SEI layer on the surface of the $ZnCo_2O_4$ particles after long-term cycling in the electrolyte with FEC. These results suggest that the addition of FEC would change the morphology of the SEI layer formed on the surface of the $ZnCo_2O_4$ particles. The formation of the uniform SEI layer could protect the $ZnCo_2O_4$ particles from aggregation and fusing. The TEM image in Fig. 5f shows that the $ZnCo_2O_4$ particles remain relatively stable with no distinct changes in their sizes and morphologies observable in the sample cycled up to 200 cycles.

Indeed, the thin SEI layer formed on the $ZnCo_2O_4$ electrode cycled in the electrolyte with FEC could be further demonstrated by the TGA curves in Fig. 6. As shown Fig. 6, the weight losses of the $ZnCo_2O_4$ electrodes after 200 discharge/charge cycles in the electrolytes with and without FEC are 1.63% and 3.92% at 400 °C, respectively, indicating less organic materials formed on the $ZnCo_2O_4$ electrode cycled in the electrolyte with FEC than those on the $ZnCo_2O_4$ electrode cycled in the electrolyte without FEC. This strongly suggests that the formation of the thinner SEI layer on the $ZnCo_2O_4$ electrode in the electrolyte with FEC.

For better understanding the influence of FEC on the SEI layer, the $ZnCo_2O_4$ electrodes cycled in the electrolytes with and without FEC are further analyzed by the XPS spectroscopy. The XPS survey spectra in Fig. 7 show the presence of C, O, F, P, Zn and Co in the both cases. The differences in the relatively atomic percentages of these elements indicate that the addition of FEC changes the chemical composition of the surface layer (Table 1). The relatively higher atomic percentages of Zn and Co in the $ZnCo_2O_4$ electrode cycled in the electrolyte with FEC, which arise from the SEI layer coated $ZnCo_2O_4$ particles, further suggest a thinner SEI layer on the $ZnCo_2O_4$ electrode. This is well consistent with the results shown in Fig. 5e and 6, where the formation of the thinner SEI layer on the $ZnCo_2O_4$ electrode cycled in the electrolyte with FEC could be demonstrated. Fig. 7b displays the deconvoluted XPS spectra of C 1s, which show the presence of four components with binding energies at 284.5, 286.0, 288.3 and 289.8 eV, corresponding to C–C, C–O, C═O, and C–F, respectively. The presence of C–O and C═O could further be demonstrated by the deconvoluted O 1s spectra in Fig. 7c, where two peaks at the binding energies of 532.5 and 531.2 eV could be clearly identified. The changes in the relative percentages of these carbon- and oxygen-containing groups, as shown in Table 1, further suggest that the addition of FEC alters the chemical composition of the SEI layer. The deconvoluted F 1s spectra in Fig. 7d show the presence of a peak corresponding to LiF, which is one of the decomposition products of $LiPF_6$.

Table 1 Element concentrations of the cycled $ZnCo_2O_4$ electrodes with and without FEC

Electrolyte	C/%	O/%	F/%	P/%	Zn/%	Co/%
Without FEC	56.47	34.06	6.20	2.42	0.79	0.05
With FEC	59.80	32.40	2.80	1.10	2.50	1.40

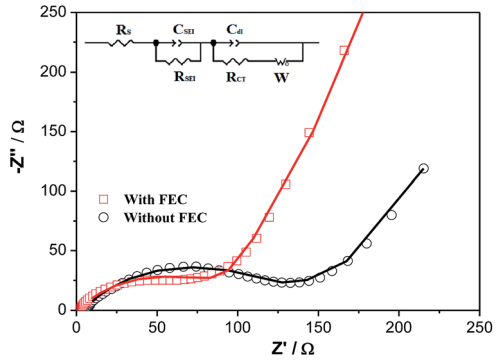

Fig. 8 Electrochemical impedance spectra of the Li/$ZnCo_2O_4$ cells in the electrolytes with and without FEC after 200 cycles. The squares and circles are the experimental data and the curves are the fitted results of the experimental data using the equivalent circuit given in the inset.

Previous work has proposed that the presence of LiF on the electrode surface would increase the interfacial impedance of the electrode materials.[50,51] According to this, the relatively low contents of LiF on the $ZnCo_2O_4$ electrode cycled in the electrolyte with FEC could be attributed to one of the possible reasons leading to the high electrochemical performance of the Li/$ZnCo_2O_4$ cells.

Fig. 8 shows the EIS spectra of the Li/$ZnCo_2O_4$ cells in the electrolytes with and without FEC after 200 cycles. As shown in the Fig. 8, the EIS spectra of the Li/$ZnCo_2O_4$ cells in the electrolytes with and without FEC both exhibit a semicircle in the high frequency region corresponding to the charge transfer processes and a sloping line in the low frequency region related to the diffusion of the lithium ions.[52,53] The fitting of the EIS spectra using the equivalent circuit given in the inset of Fig. 8 extracts the charge transfer resistance (R_{CT}) and the SEI resistance (R_{SEI}). Clearly, the Li/$ZnCo_2O_4$ cell cycled in the electrolyte with FEC exhibits much lower R_{CT} (65.5 Ω) and R_{SEI} (91.0 Ω) than those of the Li/$ZnCo_2O_4$ cell cycled in the electrolyte without FEC (R_{CT} and R_{SEI} are 124.8 Ω and 215.0 Ω, respectively). This might be due to the fact that the lower thickness of the SEI layer in the $ZnCo_2O_4$ electrode cycles in the electrolyte with FEC lowers its resistance and facilitates a ready transfer of charge across the interface of the electrolyte/SEI and SEI/$ZnCo_2O_4$. In addition to the lower R_{CT} and R_{SEI}, the Li/$ZnCo_2O_4$ cell cycled in the electrolyte with FEC also exhibit a higher diffusivity of lithium ions in the electrode, as demonstrated by its steeper sloping line in the low frequency region of the EIS spectra. This suggests that the lower thickness of the SEI layer could also accelerate the diffusion of the lithium ions through the SEI layer.

Table 2 Mass of Zn and Co deposited on the pristine lithium and the lithium electrodes in the Li/$ZnCo_2O_4$ without (Li_{-FEC}) and with FEC (Li_{+FEC})

Electrolyte	Co^{2+}/μg	Zn^{2+}/μg
Pristine lithium[a]	0.03	0.41
Li_{-FEC}	0.30	1.73
Li_{+FEC}	0.23	1.51

[a] The trace amounts of Zn and Co detected in the pristine lithium electrode might come from the impurities.

To further verify the influence of FEC on the Li/$ZnCo_2O_4$ cell, the lithium electrodes cycled in the electrolytes with and without FEC are also checked. Fig. 9 shows that the lithium electrode before cycling has a smooth and clean surface, while on the cycled electrodes some impurities could be observed. Elemental analysis could attribute these impurities to Zn and Co, which might be formed from the reduction of Zn^{2+} and Co^{2+} in the electrolytes generated from the etching of $ZnCo_2O_4$ by the reduction product of the electrolytes, HF. Indeed, the presence of Zn^{2+} and Co^{2+} in the lithium electrodes could be demonstrated by the ICP-MS analysis (Table 2). Worthnoting is that the mass of the impurities on the lithium electrode of the Li/$ZnCo_2O_4$ cell cycled in the electrolyte with FEC is much lower than that on the lithium electrode of the Li/$ZnCo_2O_4$ cell cycled in the electrolyte without FEC (as shown in Fig. 9). This might be due to the reason that the presence of FEC generates a less amount of HF or the formation of the stable SEI layers on the $ZnCo_2O_4$ electrode cycled in the electrolyte with FEC could well protect $ZnCo_2O_4$ from etching by HF.

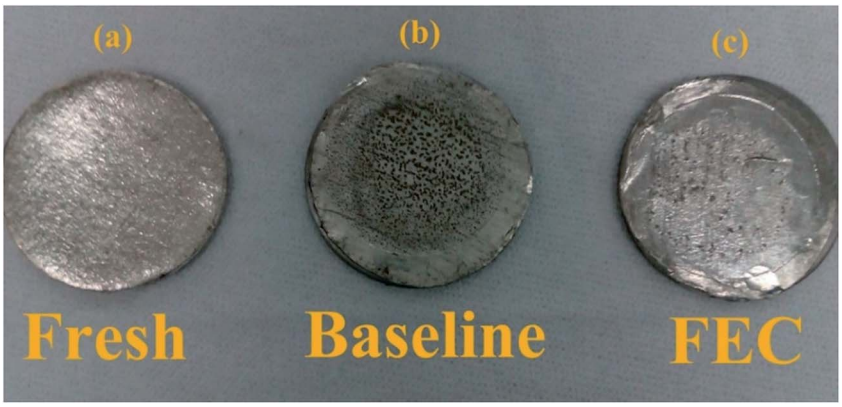

Fig. 9 Images of the pristine lithium electrode (a) and the lithium electrodes of the Li/$ZnCo_2O_4$ cells in the electrolytes without (b) and with (c) FEC after 200 cycles.

Based on the results shown above, we would attribute the high electrochemical performance of the Li/$ZnCo_2O_4$ cells in the electrolyte with FEC to the following reasons: (1) the formation of the thinner and more uniform SEI layer; (2) the low charge transfer resistance and SEI resistance; (3) the high diffusivity of lithium ions in the $ZnCo_2O_4$ electrode; (4) the presence of less LiF on the $ZnCo_2O_4$ surface; (5) the improved stability of $ZnCo_2O_4$. The thin and uniform SEI layer could facilitate the migration of lithium ions, and the low charge transfer resistance and SEI resistance and high diffusivity could increase reaction kinetics of the Li^+ storage and diffusion kinetics of the lithium ions in the electrode. The presence of less LiF on the electrode surface would decrease the interfacial impedance of the electrode materials. These, along with the high stability of $ZnCo_2O_4$ due to the formation of the stable SEI layer, lead to the LIBs with improved reversible capacity and long-term stability, as demonstrated above.

4. Conclusions

In summary, the electrochemical performance of the Li/$ZnCo_2O_4$ cell in the electrolyte with FEC has been investigated. The results show that the addition of FEC promotes the formation of more uniform and stable SEI with the thinner thickness, which could reduce the charge transfer resistance and SEI resistance, increase the diffusivity of the lithium ions of the $ZnCo_2O_4$ electrode, and improve the stability of $ZnCo_2O_4$ during the repeated discharge/charge process. In addition, the presence of FEC would lead to the formation of less LiF on the $ZnCo_2O_4$ surface, which decreases the interfacial impedance of the electrode materials. The Li/$ZnCo_2O_4$ cell in the electrolyte with FEC exhibits significantly improved irreversible capacity and long-term stability than that in the electrolyte without FEC. The formation of the thinner and more uniform SEI layer, the low charge transfer resistance and SEI resistance, the high diffusivity of lithium ions in the $ZnCo_2O_4$ electrode, the presence of less LiF on the $ZnCo_2O_4$ surface, and the improved stability of $ZnCo_2O_4$ due to the presence of the stable SEI layer could be attributed to the main reasons leading to the high electrochemical performance of the Li/$ZnCo_2O_4$ cells in the electrolyte with FEC. The work here is of great significance since it presents an addition method to fabricate LIBs with improved irreversible capacity and long-term stability and would also be helpful to promote the development of the LIB technology.

Acknowledgements

This work was financially supported by the Chinese National Natural Science Foundation (No. 11474101, and U1532139), the "Outstanding Talent and Team Plans Program" of South China University of Technology, the Zhejiang Provincial Public Welfare Technology Application Research Project (2015C31151), the Guangdong Innovative and Entepreneurial Research Team Program (No. 2014ZT05N200).

Notes and references

1 J. M. Tarascon and M. Armand, *Nature*, 2001, **414**, 359–367.
2 J. B. Goodenough and K.-S. Park, *J. Am. Chem. Soc.*, 2013, **135**, 1167–1176.
3 V. Etacheri, R. Marom, R. Elazari, G. Salitra and D. Aurbach, *Energy Environ. Sci.*, 2011, **4**, 3243.
4 M. M. Thackeray, C. Wolverton and E. D. Isaacs, *Energy Environ. Sci.*, 2012, **5**, 7854.
5 X. Liu, D. Wu, W. Ji and W. Hou, *J. Mater. Chem. A*, 2015, **3**, 968–972.
6 J. Liu, S. Tang, Y. Lu, G. Cai, S. Liang, W. Wang and X. Chen, *Energy Environ. Sci.*, 2013, **6**, 2691.
7 Y. Wu, M. Liu, H. Feng and J. Li, *Nanoscale*, 2014, **6**, 14697–14701.
8 Z. Cai, L. Xu, M. Yan, C. Han, L. He, K. M. Hercule, C. Niu, Z. Yuan, W. Xu, L. Qu, K. Zhao and L. Mai, *Nano Lett.*, 2015, **15**, 738–744.
9 Q. Su, D. Xie, J. Zhang, G. Du and B. Xu, *ACS Nano*, 2013, **7**, 9115–9121.
10 Y. Sun, X. Hu, W. Luo and Y. Huang, *J. Mater. Chem.*, 2012, **22**, 425–431.
11 H. Rong, G. Xie, S. Cheng, Z. Zhen, Z. Jiang, J. Huang, Y. Jiang, B. Chen and Z.-J. Jiang, *J. Alloys Compd.*, 2016, **679**, 231–238.
12 S. Ren, X. Zhao, R. Chen and M. Fichtner, *J. Power Sources*, 2014, **260**, 205–210.
13 J. Li, J. Wang, X. Liang, Z. Zhang, H. Liu, Y. Qian and S. Xiong, *ACS Appl. Mater. Interfaces*, 2014, **6**, 24–30.
14 D. Deng and J. Y. Lee, *Nanotechnology*, 2011, **22**, 355401.
15 B. Liu, J. Zhang, X. Wang, G. Chen, D. Chen, C. Zhou and G. Shen, *Nano Lett.*, 2012, **12**, 3005–3011.
16 Y. Qiu, S. Yang, H. Deng, L. Jin and W. Li, *J. Mater. Chem.*, 2010, **20**, 4439.
17 J. Bai, K. Wang, J. Feng and S. Xiong, *ACS Appl. Mater. Interfaces*, 2015, **7**, 22848–22857.
18 Q. Xie, F. Li, H. Guo, L. Wang, Y. Chen, G. Yue and D. L. Peng, *ACS Appl. Mater. Interfaces*, 2013, **5**, 5508–5517.
19 A. K. Rai, T. V. Thi, B. J. Paul and J. Kim, *Electrochim. Acta*, 2014, **146**, 577–584.
20 K. Schroder, J. Alvarado, T. A. Yersak, J. Li, N. Dudney, L. J. Webb, Y. S. Meng and K. J. Stevenson, *Chem. Mater.*, 2015, **27**, 5531–5542.
21 C. Xu, F. Lindgren, B. Philippe, M. Gorgoi, F. Björefors, K. Edström and T. Gustafsson, *Chem. Mater.*, 2015, **27**, 2591–2599.
22 L. Ma, H. Zhou, S. Xin, C. Xiao, F. Li and S. Ding, *Electrochim. Acta*, 2015, **178**, 767–777.
23 G. Gao, H. B. Wu, B. Dong, S. Ding and X. W. D. Lou, *Adv. Sci.*, 2015, **2**, 1400014.
24 B. Liu, X. Wang, B. Liu, Q. Wang, D. Tan, W. Song, X. Hou, D. Chen and G. Shen, *Nano Res.*, 2013, **6**, 525–534.
25 J. Bai, X. Li, G. Liu, Y. Qian and S. Xiong, *Adv. Funct. Mater.*, 2014, **24**, 3012–3020.
26 J. Li, J. Wang, D. Wexler, D. Shi, J. Liang, H. Liu, S. Xiong and Y. Qian, *J. Mater. Chem. A*, 2013, **1**, 15292.
27 Y. Sharma, N. Sharma, G. V. SubbaRao and B. V. R. Chowdari, *Adv. Funct. Mater.*, 2007, **17**, 2855–2861.
28 J. S. Chen, T. Zhu, Q. H. Hu, J. Gao, F. Su, S. Z. Qiao and X. W. Lou, *ACS Appl. Mater. Interfaces*, 2010, **2**, 3628–3635.

29 J. S. Chen and X. W. Lou, *Small*, 2013, **9**, 1877–1893.
30 C. Yuan, H. B. Wu, Y. Xie and X. W. Lou, *Angew. Chem.*, 2014, **53**, 1488–1504.
31 S. J. Harris and P. Lu, *J. Phys. Chem. C*, 2013, **117**, 6481–6492.
32 J. Luo, J. Liu, Z. Zeng, C. F. Ng, L. Ma, H. Zhang, J. Lin, Z. Shen and H. J. Fan, *Nano Lett.*, 2013, **13**, 6136–6143.
33 R. Chen, Y. Hu, Z. Shen, Y. Chen, X. He, X. Zhang and Y. Zhang, *ACS Appl. Mater. Interfaces*, 2016, **8**, 2591–2599.
34 X. Ge, Z. Li, C. Wang and L. Yin, *ACS Appl. Mater. Interfaces*, 2015, **7**, 26633–26642.
35 M. Xu, L. Zhou, Y. Dong, Y. Chen, A. Garsuch and B. L. Lucht, *J. Electrochem. Soc.*, 2013, **160**, A2005–A2013.
36 S. Zhang, M. S. Ding, K. Xu, J. Allen and T. R. Jow, *Electrochem. Solid-State Lett.*, 2001, **4**, A206.
37 A. v Cresce, S. M. Russell, D. R. Baker, K. J. Gaskell and K. Xu, *Nano Lett.*, 2014, **14**, 1405–1412.
38 K. Leung, S. B. Rempe, M. E. Foster, Y. Ma, J. M. Martinez del la Hoz, N. Sai and P. B. Balbuena, *J. Electrochem. Soc.*, 2014, **161**, A213–A221.
39 H. Rong, M. Xu, L. Xing and W. Li, *J. Power Sources*, 2014, **261**, 148–155.
40 K. Xu, *Chem. Rev.*, 2014, **114**, 11503–11618.
41 H. Rong, M. Xu, B. Xie, W. Huang, X. Liao, L. Xing and W. Li, *J. Power Sources*, 2015, **274**, 1155–1161.
42 M. D. Bhatt and C. O'Dwyer, *J. Electrochem. Soc.*, 2014, **161**, A1415–A1421.
43 E. Krämer, R. Schmitz, S. Passerini, M. Winter and C. Schreiner, *Electrochem. Commun.*, 2012, **16**, 41–43.
44 H. Rong, M. Xu, B. Xie, X. Liao, W. Huang, L. Xing and W. Li, *Electrochim. Acta*, 2014, **147**, 31–39.
45 H. A. Wilhelm, C. Marino, A. Darwiche, L. Monconduit and B. Lestriez, *Electrochem. Commun.*, 2012, **24**, 89–92.
46 L. Hu, Z. Zhang and K. Amine, *Electrochem. Commun.*, 2013, **35**, 76–79.
47 C. C. Nguyen and B. L. Lucht, *J. Electrochem. Soc.*, 2014, **161**, A1933–A1938.
48 Z. Yang, A. A. Gewirth and L. Trahey, *ACS Appl. Mater. Interfaces*, 2015, **7**, 6557–6566.
49 S. Dalavi, P. Guduru and B. L. Lucht, *J. Electrochem. Soc.*, 2012, **159**, A642.
50 L. Liao, X. Cheng, Y. Ma, P. Zuo, W. Fang, G. Yin and Y. Gao, *Electrochim. Acta*, 2013, **87**, 466–472.
51 S. J. Lee, J.-G. Han, Y. Lee, M.-H. Jeong, W. C. Shin, M. Ue and N.-S. Choi, *Electrochim. Acta*, 2014, **137**, 1–8.
52 L. Pan, X.-D. Zhu, X.-M. Xie and Y.-T. Liu, *J. Mater. Chem. A*, 2015, **3**, 2726–2733.
53 Y. Wang, G. Xing, Z. J. Han, Y. Shi, J. I. Wong, Z. X. Huang, K. K. Ostrikov and H. Y. Yang, *Nanoscale*, 2014, **6**, 8884–8890.